Discovery of a New Class of Macrocyclic Antagonists to the Human Motilin Receptor

Eric Marsault,* Hamid R. Hoveyda, Mark L. Peterson, Carl Saint-Louis, Annick Landry, Martin Vézina, Luc Ouellet, Zhigang Wang, Mahesh Ramaseshan, Sylvie Beaubien, Kamel Benakli, Sophie Beauchemin, Robert Déziel,[§] Theo Peeters,[†] and Graeme L. Fraser

Tranzyme Pharma Inc., 3001, 12e Avenue Nord, Sherbrooke, PQ, Canada, J1H 5N4

Received June 2, 2006

A novel class of macrocyclic peptidomimetics was identified and optimized as potent antagonists to the human motilin receptor (*h*MOT-R). Well-defined structure−activity relationships allowed for rapid optimization of potency that eventually led to high affinity antagonists to *h*MOT-R. Potency and antagonist functional activity were confirmed both in functional and cell-based assays, as well as on isolated rabbit intestinal smooth muscle strips. Rapid access to this novel class of macrocyclic target structures was made possible through two efficient and complementary solid-phase parallel synthetic approaches, both of which are reported herein.

Introduction

Motilin is a 22-amino acid endogenous peptide released from the endocrine cells of the gut wall and plays an important role in the regulation of intestinal motility.[1] The motilin receptor (previously called GPR38),[2] is a G-protein coupled receptor[3] predominantly expressed in the antrum, duodenum, and proximal small intestine. Activation of *h*MOT-R provokes phase III-like peristaltic contractions, as part of the migrating motor complex (MMC), a phenomenon that causes the interdigestive propulsion of gut contents along the gastrointestinal (GI) tract. As such, molecules capable of interacting with *h*MOT-R are potentially valuable for the treatment of GI disorders associated with impaired GI motility, including conditions such as IBS (irritable bowel syndrome),[4] functional dyspepsia,[5] gastroparesis,[6] and short bowel syndrome.[7]

The optimization of new motilin agonists was accelerated by the discovery that erythromycin is a potent motilin agonist, a fact responsible for the observed GI side effects of the antibiotic.[8] Analogues of erythromycin devoid of antibiotic activity were subsequently optimized as motilin agonists,[9] as well as other classes of molecules.[10] Motilin receptor antagonists, on the other hand, are fewer and have been less widely explored.[11]

We report herein results of our efforts toward the identification of potent small molecule antagonists to the *h*MOT-R. These molecules belong to the category of macrocyclic peptidomimetics and are based on the general structural motif depicted in Figure 1.

Macrocyclization has traditionally been used in peptide chemistry to restrict the conformation of linear peptides and as a means of decreasing susceptibility toward proteolytic degradation.[12] The macrocyclic structures disclosed herein are peptidomimetic in nature, with the nonpeptidic "tether" moiety being their main distinguishing feature (Figure 1). The rationale behind such a peptidomimetic structural motif was founded on the use of amino acids as a readily available pool of chiral building
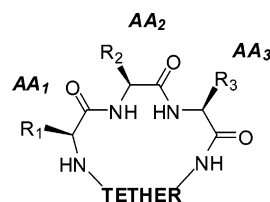

Figure 1. General structure of macrocyclic peptidomimetics (L-amino acid stereochemistry used for illustrative purposes only).

blocks, as well as for inherently relevant pharmacophoric properties for molecular recognition on GPCR targets. The tether moiety (Figure 1) was intended not only as a diversity element but, importantly, as an additional element of control to modulate the "drug likeness" of final structures. The latter aspect is achieved through the use of the tether moiety to systematically vary the conformation of the molecule as well as the relevant physicochemical properties. Thus, once in a library format, the resulting collection of macrocyclic compounds not only possesses a broad chemical diversity owing to the variety of amino acids displayed at the three positions of the peptidic moiety (aliphatic, aromatic, basic, acidic, polar, neutral), but moreover also covers a conformationally diverse space owing to the variety of tethers and their combinations with amino acids of different stereochemistry.

At the outset, approximately 10000 macrocycles from Tranzyme Pharma's proprietary library (Figure 1) were screened in a high-throughput fluorescence-based whole cell assay against the cloned human motilin receptor. Once preliminary hits were identified, the activity of the most potent compounds was in turn confirmed in binding assays (11-point curve). With the completion of this hit identification and confirmation process, compound **1** (Figure 2) was identified as a reasonably strong binding antagonist to *h*MOT-R (*K*$_i$ 137 nM, Figure 3). Subsequently, the antagonist properties of **1** were confirmed in a whole-cell assay (Figure 4).

Having identified and confirmed an antagonist to *h*MOT-R as described above, the next principal goal of the project was to establish the key structure−activity relationships (SAR) for the compound class. Once the presence of an SAR trend was
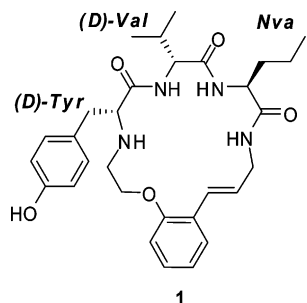
Figure 2. Structure of the Initial Motilin Antagonist Hit Obtained Through HTS.
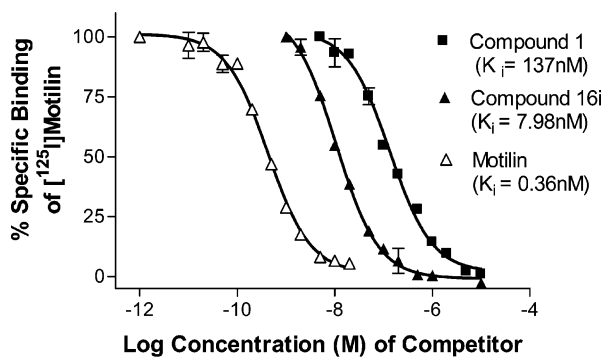

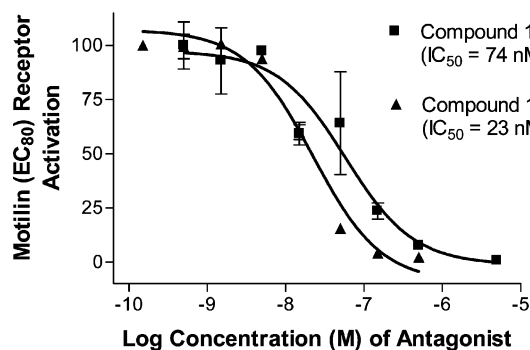**Figure 3.** Binding curves of macrocycles **1** and **16i** on *h*MOT-r.

**Figure 4.** Functional assay curves for macrocycles **1** and **16i** on *h*MOT-r.

established, as discussed in detail below, the binding affinity was further improved by using two complementary synthetic approaches.

Chemistry

Two complementary solid-phase parallel synthesis approaches were developed and utilized to access the macrocycles described herein. As such, macrocycles **1**, **12a−t**, **14d**, **14k−n**, **15a**, **16a−i**, and **17a−h** were obtained via Method A that involves macrolactamization cyclative release strategy (Scheme 1). On the other hand, macrocycles **14a−c**, **14e−i**, and **15b** were synthesized using Method B that features a ring-closing metathesis (RCM) cyclative release approach (Scheme 2). Both of these solid-phase synthetic methods allowed for systematic variations of the diversity elements in the macrocyclic structures, i.e., the three amino acids and the tether moiety (Figure 1).

In Method A (Scheme 1), PS-aminomethyl resin **2** functionalized as its 3-*S*-tritylmercapto-propionamide was used as a solid support. Initially, the trityl group was cleaved and the resulting thiol was in turn used for C-terminal amino acid attachment

Scheme 1. Synthesis of Peptidomimetic Macrocycles (macrolactamization cyclative-release, Method A)
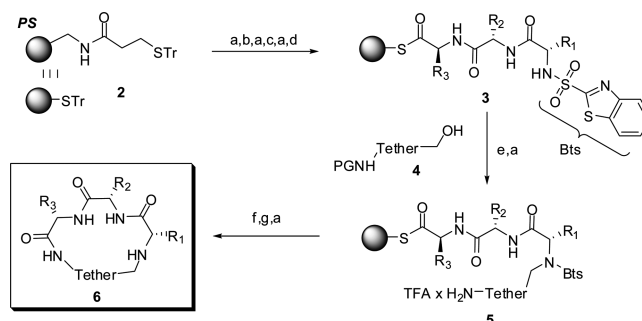
a Reagents and conditions: (a) TFA, Et₃SiH, DCM; (b) PG-AA₃-OH, PyBOP, DIPEA, NMP; (c) PG-AA₂-OH, HBTU, DIPEA, NMP; (d) Bts-AA₁-OH, HBTU, DIPEA, NMP; (e) **4**, PPh₃, DIAD, THF; (f) Ag(OCOCF₃), DIPEA, THF, MP-carbonate; (g) PS-thiophenol, KOTMS, THF:EtOH. (PG = Boc or Ddz).

Scheme 2. Synthesis of Peptidomimetic Macrocycles (RCM cyclative-release, Method B)*a*
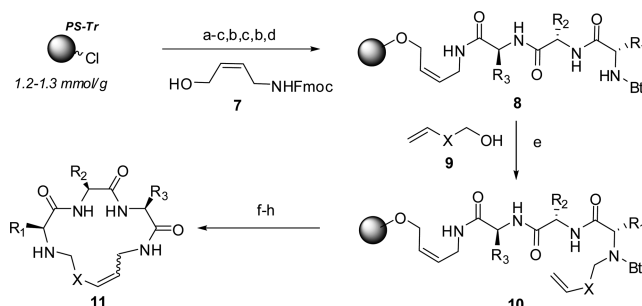
a Reagents and conditions: (a) **7**, C₅H₅N, DIPEA, THF; (b) piperidine, NMP; (c) Fmoc-AA-OH, PyBOP, DIPEA, NMP; (d) Bts-AA-OH, HBTU, DIPEA, NMP; (e) **9**, PPh₃, DIAD, THF; (f) RCM catalyst in DCM or DCE, 40 °C; (g) PS-thiophenoxide resin, THF:EtOH; (h) TFA, DCM, Et₃SiH.

and synthesis of the tripeptide fragment using Boc- and/or Ddz[13] protective groups to obtain tripeptide **3**. The third amino acid (AA₁ in Scheme 1, numbered as per standard peptide nomenclature), containing the betsyl (Bts) group,[14] was crucial in achieving efficient tether attachment (**4** in Scheme 1) through Fukuyama−Mitsunobu alkylation.[15] Tether protective group acidolysis then provided acyclic precursor **5**. Subjecting substrate **5** to silver-assisted macrolactamization under basic conditions delivered the desired macrocyclic product in solution via cyclative release.[16] An attractive feature of this cyclative release strategy, as is well documented in the literature, is its tendency to provide products with higher purity,[17] since side reactions that do not result in macrolactamization give products that remain attached to the resin.[18] The crude products thus obtained were then subjected to parallel silica gel purification. Subsequent removal of the Bts protection was performed using solid-supported potassium thiophenoxide.[19] Where necessary, side chain protective groups (such as Boc, ᵗBu esters, or ethers) were finally removed by acidolysis. Compounds were ultimately purified by MS-triggered RP-HPLC, delivering products in good purity ready for receptor binding studies.[20] This method was exploited to generate not only peptidomimetic macrocycles, but also depsipeptidomimetic macrocycles (e.g. **17a,b**), as well as compounds containing other amide bond isosteres, such as hydrazinopeptides (e.g. **17f**) and reduced amide analogues (**17e**).

The strategy for Method B is outlined in Scheme 2 and features an RCM cyclative release as the pivotal step.[21,22] Accordingly, linker **7** was attached to PS-chlorotrityl resin under

Table 1. SAR Summary for the Tripeptide Segment of Motilin Antagonist Lead Structures (**1**, Figure 2). DDL Stereochemistry Is Indicated for Reference
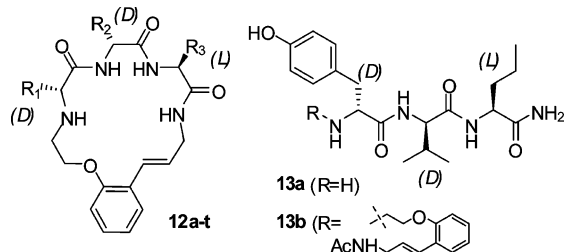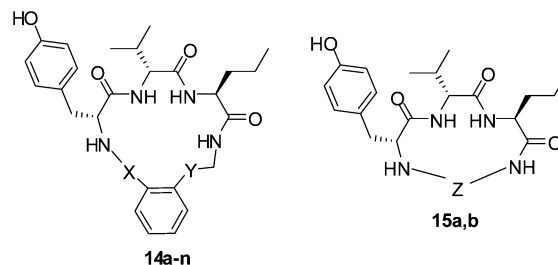

entry	AA$_1$	AA$_2$	AA$_3$	K_i (nM)
1	D-Tyr	D-Val	Nva	137
12a	D-Ala	D-Val	Nva	>10000
12b	Tyr	D-Val	Nva	>10000
12c	D-Val	D-Val	Nva	3566
12d	D-Lys	D-Val	Nva	>10000
12e	D-Glu	D-Val	Nva	>10000
12f	D-Phe	D-Val	Nva	78
12g	D-Tyr	D-Ala	Nva	196
12h	D-Tyr	Val	Nva	>10000
12i	D-Tyr	D-Glu	Nva	4898
12j	D-Tyr	D-Ser	Nva	>10000
12k	D-Tyr	D-Phe	Nva	1524
12m	D-Tyr	D-Val	Ala	1389
12n	D-Tyr	D-Val	D-Nva	335
12p	D-Tyr	D-Val	Ser	650
12q	D-Tyr	D-Val	Lys	664
12r	D-Tyr	D-Val	Asp	2553
12s	D-Tyr	D-Val	Phe	185
12t	D-Tyr	D-Val	Leu	62
13a				>10000
13b				>10000

Table 2. Summary of the Tether SAR for the Motilin Antagonist Lead Structures (**1**, Figure 2)

entry	X	Y	Z	method	K_i (nM)
1	(CH$_2$)$_2$O	(*E*) CH=CH		A	137
14a	(CH$_2$)$_3$	(*E/Z*) CH=CHCH$_2$		B	7295
14b	(CH$_2$)$_3$	(*E/Z*) CH=CH		B	>10000
14c	(CH$_2$)$_3$	(CH$_2$)$_2$		B	>10000
14d	(CH$_2$)$_3$	CH$_2$		A	>10000
14e	(CH$_2$)$_2$	(*E/Z*) CH=CHCH$_2$		B	>10000
14f	(CH$_2$)$_2$	(CH$_2$)$_3$		B	6064
14g	(CH$_2$)$_2$	(*E/Z*) CH=CH		B	9726
14h	(CH$_2$)$_2$	(CH$_2$)$_2$		B	>10000
14i	CH$_2$	(CH$_2$)$_3$		B	>10000
14k	(CH$_2$)$_4$	CH$_2$		A	6064
14m	(CH$_2$)$_2$O	(CH$_2$)$_2$		A	55
14n	(CH$_2$)$_2$O	CH$_2$		A	982
15a			(*E*)CH$_2$CH=CH(CH$_2$)$_2$	A	701
15b			(CH$_2$)$_8$	B	1197

basic conditions,[23] followed by standard Fmoc chemistry to synthesize tripeptide **8**. Similarly to Method A, the AA$_1$ amino acid was functionalized with the Bts group, and anchoring of the olefinic tether **9** was likewise effected by Fukuyama–Mitsunobu alkylation. The resulting linear alkylated tripeptide was then subjected to RCM cyclative-release to yield the macrocyclic product in solution.[24] After parallel silica gel purification, the Bts group was removed and side chains were deprotected. Where needed, the unsaturated olefin moiety formed through RCM was reduced by palladium-catalyzed hydrogenation to furnish the saturated product. Ultimately, MS-triggered RP-HPLC purification afforded macrocycles of the general structure **11**.

Results and Discussion

Tripeptide SAR. Single variations of each amino acid (AA$_1$, AA$_2$, AA$_3$, cf. Figure 1) in the tripeptide portion of the macrocyclic structures allowed us to rapidly establish the basic SAR features of this segment of the molecule. To this end, the amino acid variations applied included changes in the nature of side-chain residues, and as such, amino acids with polar, acidic, neutral, basic, hydrophobic aliphatic, and aromatic side chains were systematically screened in all three positions. Furthermore, stereochemical SAR was established through the use of D- and L-amino acids (Table 1). These modifications, as well as preliminary scanning of the tether (Table 2), were carried out in parallel using the solid-phase synthetic strategies described above to allow for higher throughput. Using both Methods A and B (vide supra), the target structures (Tables 1 and 2) were made in a single library.[25]

The specific SAR trends for the tripeptide segment of the molecule, on the basis of the radioligand binding assay against

*h*MOT-R, is as follows. At the AA$_1$ position (Figure 1), a strong preference is observed for D-amino acids bearing aromatic side-chain residues specifically (Table 1). D-Amino acids with aliphatic (**12a** and **12c**) or ionizable (**12d**–**12e**) side chains are decidedly not tolerated, nor are D-amino acids that possess aromatic side chains (e.g. **12b**). Thus, with amino acids at the AA$_1$ position bearing hydrophilic residues that are ionizable at physiological pH, such as D-Lys or D-Glu (**12d,e**), a 30- to 100-fold deterioration in receptor binding potency (K_i > 3–10 μM) was obtained. On the other hand, replacement of D-Tyr with the more lipophilic D-Phe as the AA$_1$ residue resulted in a ca. 2-fold improvement in receptor binding affinity (**1** vs **12f**). Inversion of configuration at AA$_1$ through the use of L-Tyr resulted in a complete loss of receptor binding affinity (**1** vs **12b**), indicative of a strong stereochemical preference in receptor binding for D-amino acids at AA$_1$.

With respect to the AA$_2$ residue (Figure 1), a marked preference for amino acids with aliphatic side chains in the D-configuration, such as D-Val, can be clearly detected (**1**, **12g**, Table 1). Amino acids bearing polar or ionizable residues at this position, such as D-Glu or D-Ser (**12i,j**), resulted in a 40- to 100-fold decrease in receptor binding affinity (K_i ≥ 5 μM). The stereochemical SAR at the AA$_2$ position was established through the substitution of L-Val, which abrogated receptor binding affinity (**1** vs. **12h**: K_i > 10 μM). Replacement of D-Val with D-Ala resulted in a modest decrease in potency (**12g**: K_i 196 nM). In fact, any alteration to the nature of the side-chain at the AA$_2$ position that deviated from a small aliphatic side-chain residue diminished the binding affinity significantly, demonstrating a very restrictive SAR at this position of the molecule (cf. **12i**–**k**).

In contrast, the SAR with respect to the nature of the amino acid at the AA$_3$ position (Figure 1) proved to be more permissive (Table 1). As such, amino acids with polar or ionizable side chain residues, such as Ser or Lys, resulted in a mere 5-fold decrease in potency (**1** vs **12p** or **12q**), while amino acid residues such as Phe provided similar binding potency (**1** vs **12s**). Replacement of Nva with Leu at the AA$_3$ position, resulted in

ca. two-fold potency increase (**1** vs **12t**: K_i 62 nM). Unlike the cases with the AA$_2$ and AA$_1$ positions, even the inversion of stereochemistry at the α-carbon of the AA$_3$ amino acid, through the use of D-Nva, was tolerated although less preferred (**1** vs **12n**: K_i 335 nM), since the receptor binding is diminished but not altogether abrogated as a result of this modification. Thus, in summary, position AA$_3$ permits a great deal more flexibility with respect to the nature of the side chain residue and the stereochemistry at the amino acid α-carbon, as compared to the more restrictive SAR at the AA$_1$ and AA$_2$ positions.
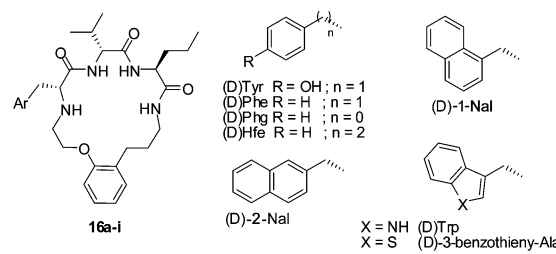
Impact of Cyclization on Activity. The critical impact of the cyclic nature of the molecule on binding was established through the use of the acyclic precursors to **1** (Table 1), both with (**13b**) and without (**13a**) the tether moiety. It is clear that the macrocyclic nature of the compound is indispensable for high binding affinity to *h*MOT-R in that neither of the acyclic analogous compounds displayed any binding to hMOT-R up to the maximum tested concentration of 10 μM (**13a,b** vs **1**).

Tether SAR. The tether portion of the macrocyclic structures (Figure 1) was also found to play a paramount role in affecting binding affinity to *h*MOT-R (**1** vs **13a,b**, Table 1). The SAR for this portion of the molecule is summarized in Table 2. To explore the tether SAR in a systematic way using focused modifications to the structure, the RCM approach (Scheme 2) was particularly effective in generating several germane analogues to the lead structure (**1**).

To begin with, the phenoxy moiety of the tether was found to be very important for receptor binding affinity: replacement of the oxygen atom by a methylene group, with or without the presence of double bond unsaturation, essentially abrogated binding (**14b,c**, Table 2). Likewise, when the aryloxy moiety was replaced in its entirety, a ca. 10-fold loss of receptor binding potency ensued (**15b**, K_i 1.2 μM, Table 2). Further, reducing the macrocycle ring size by one methylene unit in the "Y" segment of the tether (Table 2) resulted in a thorough loss of binding potency (**14d**, **14n**). The analogous modification applied to the "X" segment of the tether also resulted in 17-membered cyclic structures with very weak binding affinity for *h*MOT-R (**14e–h**, K_i > 6 μM). Moreover, binding potency was significantly compromised with the "desoxo" 18-membered ring analogues (**14e,f**). Shifting the tether phenyl ring (without the phenoxy oxygen atom) closer to the secondary amine, by two methylene units, also served to hamper receptor binding affinity (**14i**, K_i > 10 μM). A similar result was obtained with another related structural modification. Displacement of the tether phenyl ring (without the phenoxy oxygen atom) away from the secondary amine by one methylene unit also made for very weakly potent structures (**14k**, K_i 6 μM). The simplest modification turned out to be the most efficient at improving receptor binding affinity. Thus, replacement of the styrenyl unsaturation on **1** with an ethylene moiety improved potency 2.5-fold (**14m**, K_i 55 nM). This could be a useful structural modification since, a priori, removal of the electron-rich styrenyl moiety should furnish a molecule that is more resistant to oxidation and thus more suitable for drug development. Subsequently, the reduced styrenyl structure (**14m**) was used for further lead optimization (vide infra).

Reducing ring size by removing a methylene unit in the "Y" arm of the tether (Table 2), but with the phenoxy moiety of the tether intact, was also detrimental to potency (**14n**, K_i 982 nM). The indispensability of the tether phenoxy moiety to receptor binding potency was further exemplified through the results obtained with a 15-membered ring structure and an 18-membered ring analogue, in which the tether was bereft of any

Table 3. Focused Modifications to the AA$_1$ Position

entry	Ar	K_i (nM)
14m	D-Tyr	55
16a	D-Phe	57
16b	D-Cha	3247
16c	D-Phg	>10000
16d	D-Hfe	1486
16e	D-Trp	255
16f	D-2-Nal	79
16g	D-3-benzothienyl-Ala	11
16h	D-1-Nal	8.3
16i	D-Tyr(OMe)	8

aromatic moiety altogether (**15a,b**). These results demonstrated abundantly the importance of the tether phenoxy moiety as a whole, as well as the size of the ring imparted by the tether portion of the molecule, to achieving high potency binding to *h*MOT-R. In summary, the tether portion of the molecule displayed exquisite sensitivity in terms of binding potency SAR, with slight modifications in chemical nature, including those changes that affected the ring size, having a profound influence on the binding affinity to *h*MOT-R.

Focused Structural Modifications at the AA$_1$ Position. Having established the SAR in the lead structure with broad brushstrokes (vide supra), we conducted further lead optimization through the synthesis of a more narrowly focused selection of analogues by employing the aforementioned synthetic methods. The tether with the saturated styrenyl moiety (**14m**, Table 2) was established as the template for these efforts in lead optimization for the reason outlined above. Thus, combination of a saturated tether and D-Phe as the AA$_1$ amino acid (**12f**, Table 1) more than doubled the binding potency (**16a**, K_i 57 nM, Table 3) as compared to the initial lead structure **1** (K_i 137 nM, Table 2). Replacement of D-Phe with its saturated analogue, D-Cha (D-cyclohexylalanine), confirmed the absolute necessity of the presence of an aromatic moiety at the AA$_1$ position, as this change resulted in a 60-fold decrease in potency (**16b**, K_i 3.2 μM). This latter finding, combined with the indispensability of the D-configuration to obtaining high potency, suggested that the aryl side chain of the AA$_1$ residue is engaged in a π-stacking interaction with the receptor. Furthermore, either truncation or homologation of the benzyl side-chain of D-Phe, by using D-Phg and D-Hfe, respectively, resulted in a dramatically reduced binding affinity (**16c–d**, K_i > 10 μM and K_i ∼ 1.5 μM, respectively), a result that demonstrated the importance of spacing between the macrocyclic scaffold and side-chain aromatic ring when interacting with *h*MOT-R. To further probe a variety of aromatic amino acids, fused aromatic rings were investigated with the following results. Interestingly, inasmuch as D-Trp was found to be detrimental to binding (**16e**, K_i 255 nM), its isostere D-2-Nal (D-2-naphthylalanine) had little impact on affinity (**16f**, K_i 79 nM). In the same series, the isomeric D-1-Nal and its congener D-3-benzothienylalanine were found to drastically improve affinity, with equilibrium binding constants in the 10 nM range (**16g** and **16h**). On the other hand, simple O-methylation of the tyrosine phenol moiety was found

Table 4. Amide Bond Replacements and Secondary Amine Functionalization

17a-g
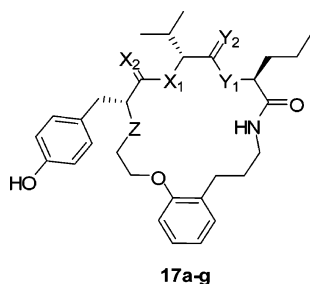
entry	X_1	X_2	Y_1	Y_2	Z	K_i (nM)
14m	NH	O	NH	O	NH	55
17a	O	O	NH	O	NH	192
17b	NH	O	O	O	NH	1876
17c	N-Me	O	NH	O	NH	>10000
17d	NH	O	N-Me	O	NH	222[a]
17e	NH	H,H	NH	O	NH	3237
17f	NH-NH	O	NH	O	NH	2373
17g	NH	O	NH	O	N-Me	2777
17h	NH	O	NH	O	N-Ac	6391

[a] Leu was used as AA_3 instead of Nva.

to bring a further 7-fold increase in potency (**16i**, K_i 8 nM). These latter results reinforced the hypothesis of a π-stacking interaction between the ligands and hMOT-R and confirmed that this part of the molecule is interacting with a particularly hydrophobic environment (**16g–i** vs **14m**) on hMOT-R.

Modifications to the Amide Bond and the Secondary Amine Moieties. Constraint-producing amino acids, such as *N*-methyl amino acids, are often used as probes for the biologically active conformation of peptides.[26] Switching the hydrogen to a methyl group in an amide bond not only affects the hydrogen bonding properties of the amide bond in question, thus potentially modulating the ligand–receptor interaction if such an interaction serves in binding the ligand to the receptor, but moreover, as is well documented, it also brings about subtle but significant structural ramifications. In the latter regard, the impact of N-methylation of an amino acid residue in a peptide chain is principally two-fold: (i) the ratio of the cis–trans rotamers of the amide bond is affected, with the relative energy of the cis isomer lowered, and (ii) the torsional ("backbone") angles are influenced with the ψ torsional angle of the *preceding* residue being the most affected.[27] The N-methylation of amino acids in the macrocyclic structure, whether at the AA_2 position (**17c**, $K_i > 10 \mu$M, Table 4) or at the AA_3 position (**17d**, K_i 222 nM, Table 4), resulted in an appreciable loss of potency, with the adverse effect at AA_2 (**17c**) particularly pronounced. These results imply that either the hydrogen of the amide serves as a pharmacophore in receptor binding (e.g., through hydrogen bonding interactions), or that the conformational restraints brought about to the macrocyclic "backbone" through N-methylation (vide supra) are detrimental to the desirable conformation of the macrocyclic ligand.

To help distinguish the cause of the adverse impact of the N-methylation on the binding affinity, the amide to ester isosteric replacement was also explored. This modification brought about the removal of the N–H portion of the amide bond without the steric bias imposed by N-methylation and its attendant effects on the "backbone" dihedral angles. The incorporation of an ester bond between AA_1 and AA_2 generated the corresponding macrocyclic depsipeptide with a four-fold decrease in binding potency (**17a** vs **14m**). Comparison of the binding potencies of **17c**, **17a**, and **14m** seemed to indicate that the amide proton

does not play a prominent role in the interaction of these molecules with the receptor. Replacement of the AA_1-AA_2 amide by the corresponding secondary amine reduced binding potency tremendously (**17e**, K_i 3.2 μM). To be noted, reduction of that amide to the amine brings about an important change in the environment, imparting on one hand more flexibility to the molecule, and, on the other hand, introducing a positive charge. Replacement of the AA_1–AA_2 amide bond by a hydrazinoam-ide[28] also led to a sharp decrease in binding (**17f**, K_i 2.4 μM).[29]

In contrast, replacement of the neighboring AA_2–AA_3 amide by an ester bond brought a 40-fold decrease in potency (**17b** vs **14m**, Table 4). This pointed to a different role for the proton of that amide, either structurally in the molecule or in regards to its interaction with the receptor. Methylation of the same amide, on the other hand, resulted in a mere 4-fold decrease in binding potency (**17d**, K_i 222 nM) with respect to **14m**. It should be kept in mind that this part of the molecule is more tolerant of important changes such as inversion of stereochemistry at the AA_3 position (for example **12n** vs **1**, Table 1) or in the nature of the amino acid.

Finally, methylation of the secondary amine in the original lead **1** also led to a sharp decrease in binding potency (**17g**, K_i 2.8 μM) and N-acetylation had an even more pronounced detrimental effect on binding (**17h**, K_i 6.4 μM). This latter observation is in agreement with the observations of Peeters et al. pointing to a direct interaction between the protonated amine moiety of both motilin and erythromycin A with residue Glu119 in the third transmembrane domain of the motilin receptor.[30]

Functional and *Ex Vivo* Assays. Figure 3 shows the binding curve of the most potent antagonists reported herein, whereas Figure 4 shows the CHO-cell functional assay results. Compounds were initially screened in competition binding assays performed on isolated membranes expressing the hMOT-R, with radioiodinated porcine motilin ($[^{125}I]$-motilin peptide) (Figure 3).

The most interesting compounds were in turn tested in an aequorin-based functional assay performed on whole CHO cells expressing the human motilin receptor (hMOT-r) (Figure 4). Inhibition of motilin-induced Ca^{2+} release was measured for all compounds. All compounds were found to be antagonists, devoid of any agonist activity at concentrations up to 10 μM.

The most potent compound **16i** was also tested in an ex vivo assay on rabbit duodenum smooth muscle strips. Briefly, isolated segments of rabbit duodenum smooth muscle were suspended in an organ chamber filled with Krebs buffer and connected to an isotonic force transducer loaded with a 1 g weight. Muscle strips were first challenged with 10^{-4} M acetylcholine until a stable maximal contraction was obtained. Afterward, a dose–response to motilin was recorded (10^{-11} to 10^{-4} M) in the presence of several concentrations of the antagonist. A Schild plot was constructed to determine that **16i** has pA_2 7.0.

Conclusion. We have identified potent macrocyclic antagonists to the human motilin receptor. As described, this compound class is characterized by well-defined SAR. These molecules hold great potential for the treatment of GI disorders associated with impaired gut motility.

Starting from an initial hit identified by high throughput screening, a rapid, 17-fold improvement in binding potency was achieved by discrete modifications on the four diversity points of the molecule. The role of amide bonds in the macrocycles was also investigated by incorporation of amide isosteric modifications.

This process was made possible by two versatile and powerful solid-phase strategies enabling the rapid, parallel synthesis of

this new class of macrocyclic peptidomimetics. More applications of this methodology will be reported in due course.

Experimental Section

Bts-protected amino acids and Bts-Cl were synthesized as reported by Vedejs et al.[14] DdzOPh, Ddz-azide, and Ddz-protected amino acids were either synthesized by the method of Birr et al.[13] or purchased directly from Advanced ChemTech (Louisville, KY) or Orpegen (Germany). Unprotected amino acids as well as Boc- and Fmoc-protected amino acids and coupling reagents were purchased from specialized amino acid manufacturers (Novabiochem, Advanced ChemTech, Bachem, Chem-Impex, Peptech).

The side chains of Tyr and Ser were protected as tBu ethers, those of Asp and Glu were protected as tBu esters, and those of Lys and Trp as Boc carbamates. In all cases where an acid-labile side-chain protective group was employed, the use of Ddz (method A) or Fmoc (method B) protection on the α-amino group allowed for orthogonal deprotection of the latter in the presence of the side chain protection. In all cases, side-chain-protected amino acids were purchased with protection in place.

Reagents and chemicals were generally purchased from Aldrich or VWR. Solvents for reactions were of DriSolv quality (anhydrous) as manufactured by EM Science. PS-aminomethyl resin functionalized with tritylmercaptopropionate linker and trityl chloride resin were purchased from Rapp Polymere (Germany). MP-carbonate and PS-thiophenol resins were purchased from Argonaut Technologies, Inc. (Foster City, CA).

The following abbreviations are used through the experimental part: DCM: dichloromethane; TFA: trifluoroacetic acid; MeOH: methanol; THF: tetrahydrofuran; NMP: *N*-methylpyrrolidinone

Representative Example of Procedure A: Synthesis of Macrocycle 16i. The synthesis was carried out in microreactors using the IRORI Minikan technology (see Supporting Information section for more details). Typically, 110 mg of PS-aminomethyl resin functionalized with an *S*-tritylmercaptopropionate linker (resin **2**) (loading: 1.2 mmol·g^{-1}) was loaded into each Minikan. Method and quantities apply to a single Minikan. In practice, multiple Minikans (generally five) were processed simultaneously to synthesize macrocycles in parallel.

Trityl Deprotection. An amount of 3.5 mL of a 10% (v/v) TFA, 5% (v/v) Et$_3$SiH solution in DCM was added to the Minikan in a glass vial, and the vial was agitated for 3 × 15 min (i.e., 3 cycles of 15 min duration) on an orbital shaker. The resin was then washed for 5 min with each of the following solvents: 3 × DCM, 3 × (DCM−MeOH 3:1), 3 × DCM. The Minikan was then dried in air (1 h) and subsequently under vacuum until full dryness was attained.

Coupling of Nva. Boc-Nva-OH (152 mg, 0.70 mmol) was added to a glass vial, followed by 3.5 mL of NMP. To this mixture was added PyBOP (346 mg, 0.66 mmol, 0.95 equiv), and the mixture was agitated until a homogeneous solution was obtained. DIPEA (183 μL, 1.05 mmol, 1.5 equiv) was then added, followed by the Minikan. The glass vial was agitated on an orbital shaker overnight. The resin was washed for 5 min periods with the following solvents: 2 × DCM, 1 × THF, 1 × NMP, 1 × (DCM−MeOH 3:1), 1 × (THF−MeOH 3:1), 1 × (DCM−MeOH 3:1), 1 × (THF−MeOH 3:1), 2 × DCM. The Minikan was then dried in air (1 h) and then under vacuum until full dryness was attained.

AA$_3$ Cleavage and Loading Quantification. To determine the effectiveness of anchoring the first amino acid, one Minikan was cleaved in order to determine the effective loading on the resin. Propylamine:THF (3 mL, 1:1 v/v) was added to the Minikan in a vial, and the mixture was agitated for 1 h. After filtration, the Minikan was washed twice for 5 min by agitating the vial with 3 mL of THF. The solvents were combined, and the filtrate was concentrated in vacuum. The residue was quantified by HPLC/CLND to give 0.11 mmol of Boc-Nva-NHPr. The effective loading of the resin thus became 1.0 mmol·g^{-1}, or 83% of the initial theoretical resin loading.

Capping the Resin. A volume of 3.5 mL of a DCM−Ac$_2$O−DIPEA (20:5:1, v/v/v) solution was added to the Minikan in a glass vial, and the vial was agitated on an orbital shaker for 1 h. The resin was washed for 5 min periods with the following solvents: 3 × DCM, 3 × (DCM−MeOH 3:1), 3 × DCM. The Minikan was then dried in air (1 h) and then under vacuum until full dryness was attained.

Boc Deprotection.[31] 3.5 mL of a 33% TFA, 3% Et$_3$SiH (v/v) solution in DCM was added to the Minikan in a glass vial, and the vial was agitated for 1 h on an orbital shaker. The resin was then washed for 5 min periods with the following solvents: 3 × DCM, 3 × (DCM−MeOH 3:1), 3 × DCM. The Minikan was dried in air (1 h) and then under vacuum until full dryness was attained.

Coupling of Boc-D-Val-OH. Boc-D-Val-OH (152 mg, 0.7 mmol) was added to a glass vial, followed by 3.5 mL of NMP. To this mixture was added HBTU (252 mg, 0.66 mmol, 0.95 equiv), and the resulting mixture was agitated until a homogeneous solution was obtained. DIPEA (183 μL, 1.05 mmol, 1.5 equiv) was added, followed by the Minikan. The glass vial was agitated on an orbital shaker overnight. The resin was washed for 5 min periods with the following solvents: 2 × DCM, 1 × THF, 1 × NMP, 1 × (DCM−MeOH 3:1), 1 × (THF−MeOH 3:1), 1 × (DCM−MeOH 3:1), 1 × (THF−MeOH 3:1), 2 × DCM. The Minikan was first dried in air (1 h) and then under vacuum until full dryness was attained.

Boc Deprotection.[32] As indicated above.

Coupling of Bts-(D)Tyr(OMe)-OH. Bts-(D)Tyr(OMe)-OH (277 mg, 0.7 mmol) was added to a glass vial, followed by 3.5 mL of NMP. To this mixture was added HBTU (252 mg, 0.66 mmol, 0.95 equiv), and the resulting mixture was agitated until a homogeneous solution was obtained. DIPEA (183 μL, 1.05 mmol, 1.5 equiv) was added, followed by the Minikan. The glass vial was agitated on an orbital shaker overnight. The resin was washed for 5 min periods with the following sequence: 2 × DCM, 1 × THF, 1 × NMP, 1 × (DCM−MeOH 3:1), 1 × (THF−MeOH 3:1), 1 × (DCM−MeOH 3:1), 1 × (THF−MeOH 3:1), 2 × DCM. The Minikan was dried in air (1 h) and then under vacuum until full dryness was attained.

Tether 4 Attachment. Boc-protected tether alcohol **4b**[33] (219 mg, 0.75 mmol) was added to a glass vial, followed by 3.5 mL of THF. To this mixture was added triphenylphosphine (197 mg, 0.75 mmol, 1.0 equiv), and the resulting mixture was stirred until a homogeneous solution was obtained. The Minikan was then added to the solution, followed by DIAD (148 μL, 0.75 mmol, 1.0 equiv). The resultant reaction mixture was agitated on an orbital shaker overnight. The resin was then washed for 5 min cycles with the following solvents: 2 × DCM, 1 × Toluene, 1 × EtOH, 1 × Toluene, 1 × (DCM−MeOH 3:1), 1 × (THF−MeOH 3:1), 1 × (DCM−MeOH 3:1), 1 × (THF−MeOH 3:1), 2 × DCM. The Minikan was dried in air (1 h) and then under vacuum until full dryness was attained.

Boc Deprotection.[34] See above.

Macrocyclization. An amount of 65 mg of MP-carbonate resin (0.18 mmol) was weighed into a 4 mL glass vial. The Minikan was opened and its contents transferred to the vial, followed by addition of Ag(OCOCF$_3$) (29 mg, 0.13 mmol, 1.0 equiv). Finally, 1.5 mL anhydrous THF was added, followed by DIPEA (50 mL, 0.29 mmol). The reaction mixture was agitated on an orbital shaker at ambient temperature overnight. The solution was then filtered and the resin washed with THF (2 × 2 mL). The crude macrocycle was then coarsely purified by silica gel chromatography on an ISCO Combiflash (DCM−MeOH 95:5) and then used as such for the following step.

Bts Deprotection.[35] The Bts-protected macrocycle was dissolved in 1.4 mL of a THF−EtOH 95% (1:1, v/v) in a 4 mL glass vial. An amount of 160−180 mg of PS-thiophenoxide resin was added (0.22−0.25 mmol, approximately 20 equiv) to the vial. The solution was then agitated on an orbital shaker for 2 h. The solution was filtered into another glass vial, and the resin was rinsed with a THF−EtOH 95% solution (1:1 v/v, 2 × 2 mL). After combination of the organic phases, the volatiles were removed under vacuum. The amount of macrocycle in the crude was quantified using an

HPLC−CLND detector, and found to be 13 mg (21% overall yield based on the effective loading of Nva).

RP-HPLC Purification. Crude macrocycle **16i** was purified on a Waters FractionLynx MS-triggered reverse phase preparative system, using a water:methanol gradient containing 0.1% TFA as the eluent. Macrocycle **16i** was obtained as a colorless film (5.2 mg as quantified by HPLC−CLND). HPLC purity: 98.8% (UV detector), 100% (ELSD detector), 100% (CLND detector). HRMS: $C_{31}H_{44}N_4O_5$, calc: 552.3311, found: 552.3321 ± 0.0016. ^{1}H NMR (300 MHz, CD$_3$OD) δ (ppm) 8.77 (d, 1H, 9 Hz); 7.75 (d, 1H, 3 Hz); 7.21−7.05 (m, 4H); 6.87−6.73 (m, 4H); 4.46−4.38 (m, 1H); 4.15−4.00 (m, 3H); 3.79 (d, 1H, 12 Hz); 3.74 (s, 3H); 3.29−3.04 (m, 5H); 2.71 (dt, 1H, 12 Hz; 6 Hz); 2.63−2.53 (m, 1H); 2.20 (dt, 1H, 12 Hz; 3 Hz); 2.13−1.98 (m, 2H); 1.66−1.33 (m, 5H); 1.12 (s, 3H, 6 Hz); 1.02 (d, 3H, 6 Hz); 0.96 (t, 3H, 6 Hz). ^{13}C NMR (75.5 MHz, CD$_3$OD) δ (ppm) 174.80; 174.21; 160.44; 127.31; 132.47; 131.46; 131.32; 128.43; 122.11; 114.89; 111.41; 65.88; 63.69; 61.48; 55.59; 54.20; 48.10; 42.40; 38.48; 34.31; 31.32; 30.09; 29.08; 20.57; 20.26; 19.52; 13.67.

Typically, compounds were obtained as TFA salts. They were dissolved at 10 mM concentration in DMSO in a 96-well plates and stored at −60 °C until tested. For characterization purposes, selected macrocycles underwent a salt exchange step using ion-exchange resin to generate the corresponding hydrochloride salts.

Supporting Information Available: Experimental procedures for biological assays; the synthesis of macrocycles (method B), including procedures for the synthesis of tether and linker building blocks; characterization data for building blocks (LC/MS, ^{1}H, NMR, ^{13}C NMR) and macrocycles (HPLC/MS, HRMS, ^{1}H NMR, ^{13}C NMR), including spectra and chromatograms. This material is available free of charge via the Internet at http://pubs.acs.org.

References

(1) Brown, J. C.; Mutt, V.; Dryburgh, J. R. Motilin, a Gastric Activity Stimulating Polypeptide: The Complete Amino Acid Sequence. *Can. J. Biochem.* **1973**, *51*, 533−537.

(2) Feighner, S. D.; Tan, C. P.; McKee, K. K.; Palyha, O. C.; Hreniuk, D. L.; Pong, S. S.; Austin, C. P.; Figueroa, D.; MacNeil, D.; Cascieri, M A.; Nargund, R.; Bakshi, R.; Abramovitz, M.; Stocco, R.; Kargman, S.; O'Neill, G.; Van Der Ploeg, L. H T.; Evans, J.; Patchett, A. A.; Smith, R. G.; Howard, A. D. Receptor for Motilin Identified in the Human Gastrointestinal System. *Science* **1999**, *284*, 2184−2188.

(3) For a review on motilin and potential applications, please refer to Itoh, Z. Motilin and clinical application. *Peptides* **1997**, *18*, 593−608.

(4) (a) Sjölund, K.; Ekman, R.; Lindgren, S.; Rehfeld, J. F. Disturbed Motilin and Cholecystokinin Release in the Irritable Bowel Syndrome. *Scand. J. Gastroenterol.* **1996**, *31*, 1110−1114. (b) Simrén, M.; Björnsson, E. S.; Abrahamsson, H. High Interdigestive and Postprandial Motilin Levels in Patients with the Irritable Bowel Syndrome. *Neurogastroenterol. Motil.* **2005**, *17*, 51−57.

(5) (a) Malagelada, J. R. Gastrointestinal Motor Disturbances in Functional Dyspepsia. *Scand. J. Gastroenterol. Suppl.* **1991**, *182*, 29−32. (b) Kamerling, I. M. C.; van Haarst, A. D.; Burggraaf, J.; de Kam, M.; Biemond, I.; Jones, R.; Cohen, A. F.; Masclee, A. A. M. Exogenous Motilin Affects Postprandial Proximal Gastric Motor Function and Visceral Sensation. *Dig. Dis. Sci.* **2002**, *47*, 1732−1736. (c) Cuomo, R.; Vandaele, P.; Coulie, B.; Peeters, T.; Depoortere, I.; Janssens, J.; Tack, J. Influence of Motilin on gastric Fundus Tone and on Meal-Induced Satiety in Man: Role of Cholinergic Pathways. *Am. J. Gastroenterol.* **2005**, *100*, 1−8.

(6) (a) Cowles, V. E.; Nellans, H. N.; Seifert, T. R.; Besecke, L. M.; Segreti, J. A.; Mohning, K. M.; Faghih, R.; Verlinden, M. H.; Wegner, C. D. Effect of Novel Motilide ABT-229 versus Erythro-

mycin and Cisapride on gastric Emptying in Dogs. *J. Pharm. Exp. Ther.* **2000**, *293*, 1106−1111. (b) Russo, A.; Stevens, J. E.; Giles, N.; Krause, G.; O'Donovan, D. G.; Horowitz, M.; Jones, K. L. A. Effect of the Motilin Agonist KC11458 on Gastric Emptying in Diabetic Gastroparesis. *Aliment. Pharmacol. Ther.* **2004**, *20*, 333−338.

(7) For a review on short bowel syndrome, see Nightindale, J. M. D. Management of Patients with a Short Bowel. *World J. Gastroenterol.* **2001**, *7*, 741−751.

(8) Peeters, T.; Matthijs, G.; Depoortere, I.; Cachet, T.; Hoogmartens, J.; Vantrappen, G. Erythromycin is a motilin receptor agonist. *Am. J. Physiol.* **1989**, *257*, G470−4.

(9) (a) Lartey, P. A.; Nellans, H. N.; Faghih, R.; Petersen, A.; Edwards, C. M.; Freiberg, M.; Quigley, S.; Marsh, K.; Klein, L. L.; Plattner, J. J. Synthesis of 4″-Deoxy Motilides: Identification of a potent and Orally Active Prokinetic Drug Candidate. *J. Med. Chem.* **1995**, *38*, 1793−1798. (b) Peeters T. L. GM-611. *Curr. Opin. Investig. Drugs* **2001**, *2*, 555−557. (c) for a historical perspective on the development of motilin agonists, please refer to T. L. Peeters. New Motilin Agonists: a Long and Winding Road. *Neurogastroenterol. Motil.* **2006**, *18*, 1−5.

(10) Li, J. J.; Chao, H. G.; Wang, H.; Tino, J. A.; Laurence, M.; Ewing, W. R.; Ma, Z.; Yan, M.; Slusharchyk, D.; Seethala, R.; Sun, H.; Li, D.; Burford, N. T.; Stoffel, R. H.; Salyan, M. E.; Li, C. Y.; Witkus, M.; Zhao, N.; Rich, A.; Gordon, G. A. Discovery of a Potent and Novel Motilin Agonist. *J. Med. Chem.* **2004**, *47*, 1704−1708.

(11) For precedents on the identification of motilin receptor antagonists belonging to different chemical classes, please refer to (a) Poitras, P.; Miller, P.; Gagnon, D.; St-Pierre, S. Motilin Synthetic Analogues and Motilin Receptor Antagonists. *Biochem. Biophys. Res. Commun.* **1994**, *205*, 449−454. (b) Haramura, M.; Okamachi, A.; Tsuzuki, K.; Yogo, K.; Ikuta, M.; Kozono, T.; Takanashi, H.; Murayama, E. Design and Synthesis of N-Terminal Cyclic Motilin Partial Peptides: a Novel Pure Motilin Antagonist. *Chem. Pharm. Bull.* **2001**, *49*, 40−43. (c) Beavers, M. P.; Gunnet, J. W.; Hageman, W.; Miller, W.; Moore, J. B.; Zhou, L.; Chen, R. H. K.; Xiang, A.; Urbanski, M.; Combs, D. W.; Mayo, K. H.; Demarest, J. Discovery of the First Non-peptide Antagonist to the Motilin Receptor. *Drug Des. Discovery* **2001**, *17*, 243−251. (d) Takanashi, H.; Yogo, K.; Ozaki, K. I.; Ikuta, M.; Akima, M.; Koga, H.; Nabata, H. GM-109: A Novel, Selective Motilin Receptor Antagonist in the Smooth Muscle of the Rabbit Small Intestine. *J. Pharm. Exp. Ther.* **1995**, *273*, 624−628.

(12) For reviews, see (a) Li, P.; Roller, P. Cyclization Strategies in Peptide Derived Drug Design. *Curr. Top. Med. Chem.* **2002**, *2*, 325−341. (b) Lambert, J. N.; Mitchell, J. P.; Roberts, K. D. The Synthesis of Cyclic Peptides. *J. Chem. Soc., Perkin Trans. 1* **2001**, 471−484. (c) McGeary, R. P.; Fairlie, D. P. Macrocyclic Peptidomimetics: Potential for Drug Development. *Curr. Opin. Drug Discuss. Dev.* **1998**, *1*, 208−217. (d) Goodman, M.; Ro, S. Peptidomimetics for Drug Design. In *Burger's Medicinal Chemistry and Drug Discovery*; Wiley: New York, 1995; Vol. 1, pp 803−861.

(13) Birr, C.; Lochinger, W.; Stahnke, G.; Lang, P. Der α,α-Dimethyl-3,5-Dimethoxybenzyloxycarbonyl (Ddz)-Rest, eine Photo- und Saürelabile Stickstoff-Schutzgruppe für die Peptidchemie. *Liebigs Ann. Chem.* **1972**, *763*, 162−172.
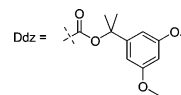
(14) For more details on the discovery and chemistry of the Bts protective group, see Vedejs, E.; Lin, S.; Klapars, A.; Wang, J. Heteroarene-2-Sulfonyl Chlorides (BtsCl:ThsCl): Reagents for Nitrogen Protection and >99% Racemization-Free Phenylglycine Activation with SOCl$_2$. *J. Am. Chem. Soc.* **1996**, *118*, 9796−9799.

(15) Fukuyama, T.; Cheung, M.; Jow, C. K.; Hidai, Y.; Kan, T. 2,4-Dinitrobenzenesulfonamides: a Simple and Practical Method for the Preparation of a Variety of Secondary Amines and Diamines. *Tetrahedron Lett.* **1997**, *38*, 5831−5834.

(16) (a) Macrolactamization by thioester aminolysis has been performed by thioesterase, see for example Boddy, C. N. Sweetening Cyclic Peptides Libraries. *Chem. Biol.* **2004**, *11*, 1599−1600 and references therein. (b) The thioester linkage also forms the basis of the native ligation of peptides, see Dawson, P. E.; Muir, T. W.; Clark-Lewis, I.; Kent, S. B. H. Synthesis of Proteins by Native Chemical Ligation. *Science* **1994**, *266*, 776−779. (c) For macrocyclization using thioester aminolysis in the presence of silver, see Zhang, L.; Tam, J. P. Lactone and Lactam Library Synthesis by Silver Ion-Assisted Orthogonal Cyclization of Unprotected Peptides. *J. Am. Chem. Soc.* **1999**, *121*, 3311−3320.

(17) Average crude purity 70% (HPLC−UV).

(18) For examples of macrocyclization/release strategies other than RCM, see (a) Li, W.; Burgess, K. A New Solid-Phase Linker for Suzuki Coupling with Concomitant Macrocyclization: Synthesis of β-Turn Mimics. *Tetrahedron Lett*. **1999**, *40*, 6527−6530. (b) Nicolaou, K. C.; Pastor, J.; Winssinger, N.; Murphy, F. Solid-Phase Synthesis of Macrocycles by an Intramolecular Ketophosphonate Reaction. Synthesis of a (*dl*)-Muscone Library. *J. Am. Chem. Soc*. **1998**, *120*, 5132−5133. (c) La Porta, E.; Piarulli, U.; Cardullo, F.; Paio, A.; Provera, S.; Seneci, P.; Gennari, C. Cyclative Cleavage via Solid Phase Supported Stabilized Sulfur Ylides: Synthesis of Macrocyclic Lactones. *Tetrahedron Lett*. **2002**, *43*, 761−766. (d) Shigenaga, A.; Moss, J. A.; Ashley, F. T.; Kaufmann, G. F.; Janda, K. D. Solid-Phase Synthesis and Cyclative Cleavage of Quorum Sensing Depsipeptide Analogues by Acylphenyldiazene Activation. *Synlett* **2006**, *4*, 551−554. (e) Pernerstorfer, J.; Kramer, T. Solid-Phase Chemistry: Cyclative Cleavage: a Versatile Concept in Solid-Phase Organic Chemistry. *Methods Princ. Med. Chem*. **2000**, *9*, 99−122.

(19) Wuts, P. G. M.; Gu, R. L.; Northuis, J. M.; Thomas, C. L. A New Method for Deprotection of Benzothiazolesulfonamides Using a Thiol and a Base. *Tetrahedron Lett*. **1998**, *39*, 9155−9156.

(20) QC criteria (RP-HPLC) were >85% (UV), >90% (CLND), >95% (ELSD).

(21) For precedents of cyclative release by RCM from solid support, please refer to (a) Pernerstorfer, J.; Schuster, M.; Blechert, S. Cyclization/ Cleavage of Macrocycles by Ring-Closing Metathesis on Solid Support− Conformational Studies. *Chem. Commun*. **1997**, 1949− 1950. (b) Piscopio, A. D.; Miller, J. F.; Koch, K. Ring Closing Metathesis in Organic Synthesis: Evolution of a High Speed, Solid-Phase Method for the Preparation of β-Turn Mimetics. *Tetrahedron* **1999**, *55*, 8189−8198. (c) Veerman, J. J. N.; van Maarseveen, J. H.; Visser, G. M.; Kruse, C. G.; Schoemaker, H. E.; Hiemstra, H.; Rutjes, F. P. J. T. Ring-Closing Metathesis on Solid Support: Elaboration of a Cyclization/Cleavage Strategy Towards Unsaturated α-Esters-Substituted N-Heterocycles. *Eur. J. Org. Chem*. **1998**, 2583−2589. (d) Sasmal, S.; Geyer, A.; Meier, M. E. Synthesis of Cyclic Peptidomimetics from Aldol Building Blocks. *J. Org. Chem*. **2002**, *67*, 6260. (e) Timmer, M. S. M.; Codée, J. D. C.; Overkleeft, H. S.; van Boom, J. H.; van der Marel, G. A. A Tandem Ring-Closing Metathesis Cleavable Linker System for Solid-Phase Oligosaccharide Synthesis. *Synlett* **2004**, *12*, 2155−2158.

(22) For selected examples of macrocyclic peptidomimetics obtained by RCM, see (a) Blackwell, H. E.; Sadowsky, J. D.; Howard, R. J.; Sampson, J. N.; Chao, J. A.; Steinmetz, W. E.; O'Leary, D. J.; Grubbs, R. H. Ring-Closing Metathesis of Olefinic Peptides: Design, Synthesis, and Structural Characterization of Macrocyclic Helical Peptides. *J. Org. Chem*. **2001**, *66*, 5291−5302. (b) Barrett, A. G. M.; Hennessy, A. J.; Le Vézouët, R.; Procopiou, P. A.; Seale, P. W.; Stefaniak, S.; Upton, R. J.; White, A. J. P.; Williams, D. J. Synthesis of Diverse Macrocyclic Peptidomimetics Utilizing Ring-Closing Metathesis and Solid-Phase Synthesis. *J. Org. Chem*. **2004**, *69*, 1028−1037. (c) Shi, Z. D.; Lee, K.; Wei, C. Q.; Roberts, L. R.; Worthy, K. M.; Fisher, R. J.; Burke, T. R. Synthesis of a 5-methylindolyl-Containing Macrocycle that Displays Ultrapotent Grb2 SH2 Domain-Binding Affinity. *J. Med. Chem*. **2004**, *47*, 788−791. (d) Prabhakaran, E. N.; Nageswara Rao, I.; Boruah, A.; Iqbal, J. Synthesis of Small Cyclic Peptides via Reverse Turn Induced Ring Closing Metathesis of Tripeptides. *J. Org. Chem*. **2002**, *67*, 8247−8250. (e) Lee, D.; Sello, J. K.; Schreiber, S. L. A Strategy for Macrocyclic Ring Closure and Functionalization Aimed Toward Split-Pool Syntheses. *J. Am. Chem. Soc*. **1999**, *121*, 10648−10649. (f) Hi, X.; Nguyen, K. T.; Verlinde, C. L. M. J.; Hol, W. G. J.; Pei, D. Structure-Based Design of a Macrocyclic Inhibitor for Peptide Deformylase. *J. Med. Chem*. **2003**, *46*, 3771−3774.

(23) For a rapid synthesis of linker via cross metathesis, please refer to Hoveyda, H.; Vézina, M. Synthesis of Unsaturated Amino Alcohols Through Unexpectedly Selective Ru-Catalyzed Cross-Metathesis Reactions. *Org. Lett*. **2005**, *7*, 2113−2116.

(24) RCM catalysts (see structures below) used in method B are second generation catalysts from (a) Grubbs et al., see Scholl, M.; Ding, S.; Lee, C. W.; Grubbs, R. H. Synthesis and Activity of a New Generation of Ruthenium-Based Metathesis Coordinated with 1,3-

Dimesityl-4,5-dihydroimidazol-2-ylidene Ligands. *Org. Lett*. **1999**, *1*, 953−956; and (b) Hoveyda et al., see Kingsbury, J. S.; Harrity, J. P. A.; Bonitatebus, P. J.; Hoveyda, A. H. A Recyclable Ru−Based Metathesis Catalyst. *J. Am. Chem. Soc*. **1999**, *121*, 791−799.

Grubbs 2nd generation catalyst   Hoveyda 2nd generation catalyst
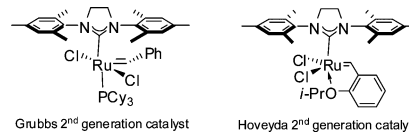
(25) Macrocycles were synthesized in library format and purified by MS-triggered preparative HPLC. Purity and identity was ascertained by HPLC-MS using three detection methods: UV, Evaporative Light-Scattering Detector (ELSD) and ChemiLuminsecent Nitrogen Detector (CLND). The latter receptor was also used for quantification of compounds. Macrocycles were further characterized by HRMS. Selected macrocycles were further characterized by ^{1}H and ^{13}C NMR. All characterization descriptions and raw data are available in the Supporting Information section.

(26) For a review on the influence of N-methylation of amino acids on structure and function of biologically active peptides, please refer to Sagan, S.; Karoyan, P.; Lequin, O.; Chassaing, G.; Lavielle, S. N- and C α-Methylation in Biologically Active Peptides: Synthesis, Structural and Functional Aspects. *Curr. Med. Chem*. **2004**, *11*, 2799−2822.

(27) *N*-Methyl amino acids can also impart increased resistance to proteolysis and have been thus used, for instance, in the design of metabolically stable renin inhibitors, see Pals, D. T.; Thaisrivongs, S.; Lawson, J. A.; Kati, W. M.; Turner, S. R.; DeGraaf, G. L.; Harris, D. W.; Johnson, G. A. An Orally Active Inhibitor of Renin. *Hypertension* **1986**, *8*, 1105−1112.

(28) Günther, R.; Hofman, H. J. Hydrazino Peptides as Foldamers: an Extension of the β-Peptide Concept. *J. Am. Chem. Soc*. **2001**, *123*, 247−255. For the synthesis of hydrazino-D-Val, the method reported by Vidal *et al.* was used with modifications, see Guy, L.; Vidal, J.; Collet, A. Design and Synthesis of Hydrazinopeptides, and Their Evaluation as Human Leukocyte Elastase Inhibitors. *J. Med. Chem*. **1998**, *41*, 4833−4843 and Supporting Information section for modifications.

(29) Note that the macrocycle resulting from the replacement of amide by hydrazinoamide is a 19-membered ring instead of an 18-membered ring.

(30) Xu, L.; Depoortere, I.; Vertongen, P.; Waelbroeck, M.; Robberecht, P.; Peeters, T. L. Motilin and Erythromycin-A Share a Common Binding Site in the Third Transmembrane Segment of the Motilin Receptor. *Biochem. Pharm*. **2005**, *70*, 879−887.

(31) In the case of Ddz side chain deprotection, the substrate was treated with 2% TFA, 3% Et$_3$SiH, DCM for 15 min and the Minikan was washed similarly.

(32) In the case of Ddz deprotection, the resin was treated with 1% TFA, 3% Et$_3$SiH in DCM for 3 cycles of 15 min and washed as indicated.

(33) Please refer to the Supporting Information section for the synthesis and numbering of tether building blocks.

(34) In the case of Ddz deprotection, a 2% TFA, 3% Et$_3$SiH solution in DCM was used for 1 h.

(35) Preparation of PS-thiophenoxide resin (1 g of resin): 1 g of PS-thiophenol resin was added to 30 mL of THF−EtOH 95% (1:1, v/v), followed by addition of potassium trimethylsilanolate (0.19 g, 1.5 mmol, 1.1 equiv). The mixture was agitated for 1 h under nitrogen on an orbital shaker. The resin was filtered and washed thoroughly (5 × 15 mL) with THF−EtOH 95% (1:1, v/ v), followed by THF (5×). The resin was transferred to a round-bottom flask and then dried with a heat gun under vacuum until fully dry.

(36) Abbreviations: Bts, betsyl, or benzothiazol-2-sulfonyl; *h*MOT-R, human motilin receptor; MMC, migrating motor complex; GPCR, G-protein coupled receptor; GI, gastro-intestinal; IBS, irritable bowel syndrome; PS, polystyrene resin; RP-HPLC, reverse phase high performance liquid chromatography; AA, amino acid; MP, macroporous polystyrene resin.